



# Topology Optimization for Additive Manufacturing: Considering Maximum Overhang Constraint

Andrew T. Gaynor\* and James K. Guest<sup>†</sup>

*Johns Hopkins University, Baltimore, MD, 21218, USA*

Additively manufactured components often require temporary support material during the 3D printing process. In the case of polymer material process such as Fuse Deposition Modeling (FDM), the support material can be dissolved away. However in the case of metals in a selective laser melting (SLM) process, the support and component material are one in the same. Since the support structure adds both material cost and post-processing cost to every component printed, it is desired to limit or completely eliminate the need for such material. As such, it is proposed to take advantage of the maximum printable overhang angle (the angle at which the AM process requires no support material) by harnessing topology optimization as the design engine. This is accomplished through a topology optimization projection scheme, in which the angle constraint is imposed through a Heaviside projection and not applied as an explicit constraint. Solutions to two standard topology optimization problems are included and show good agreement with the overhang constraint.

## Nomenclature

$d$	Displacements
$F$	Vector of nodal forces
$f$	Objective function
$H$	Heaviside operator
$K$	Global Stiffness Matrix
$V$	Total Volume Allowed
$v$	Volume of every element
$\eta$	SIMP exponent
$\psi$	Design variable
$\phi$	Print head location variable
$\rho$	Element density
$\Omega$	Domain

## I. Introduction

Additive manufacturing (AM) is free-form manufacturing technique in which a component is built from bottom up in a layer by layer manner. Unlike more traditional manufacturing techniques such as milling or casting, AM allows for much greater design freedom. In order to truly exploit the new design freedom, the engineer must reimagine the topology of the component, as previously unattainable geometries are now an option. For this reason topology optimization is a perfect design tool for AM.

Topology optimization is a free-form material distribution scheme in which the user defines an objective function to minimize (such as compliance) subject to a certain constraints. While conceptually simple, there exist a number of numerical challenges associated with topology optimization. These include elimination of

\*Graduate Research Assistant, Department of Civil Engineering, 3400 N. Charles St., Baltimore, MD, 21218, AIAA Student Member.

<sup>†</sup>Associate Professor, Department of Civil Engineering, 3400 N. Charles St., Baltimore, MD, 21218, AIAA Member.

checkerboard solutions, the formation of one-node hinges and mesh dependency. For further discussion of such topics, the reader is referred to work by Sigmund and Bendsoe.<sup>1,19</sup>

Additive manufacturing, while seemingly a free-form manufacturing technique, does have a few design limitations. These are primarily: no internal voids are allowed and support material is necessary for many structures. This paper will focus on designing AM components to eliminate the need for support material. Both polymer based processes such as Fused Deposition Modeling (FDM)<sup>12</sup> and powdered metal based processes such as selective laser melting (SLM) require support material in order to manufacture certain parts. In the case of FDM, there is often a soluble support material which can easily be removed in a post-print liquid bath. As for metal support material, the process is a bit more complicated, as the support metal must be chipped or grinder off the part after the printing process.

Metal support material is essential for many reasons identified by Hussein et al.<sup>14</sup> These include ease of part removal, anchorage to platform during build process, preventing the toppling of thin-walled sections during the powder wiper process, and preventing the curling and distortion from melting and solidifying process. Vandenbrouke et al. goes into depth on the curling and distortion topic.<sup>22</sup> Mercelis et al. details the consequences of residual stresses due to the heating and cooling phenomenon, particularly pointing to issues of warpage and cracks.<sup>16</sup>

Several researchers have identified the maximum achievable overhang angle. Xu et al. identified the issue in bioprinting applications, where going past the max angle resulted in failure due to moment imbalance and droplet impact-induced crash, and proposed a scaffold free printing process which limited the overhang angle.<sup>23</sup> Recently, Brackett et al. identified the problem and suggested using topology optimization in conjunction with a heuristic penalization scheme on angles greater than the maximum allowable.<sup>3</sup> Alternatively, Hussein et al. proposed using low volume lattices as support material in order to reduce the volume of material used in the print process.<sup>14</sup> Others have also suggested strategies to minimize and eliminate support material.<sup>5,17</sup> Notably, Thomas identified 45° as the typical maximum achievable overhang angle.<sup>21</sup>

Geometry control in topology optimization is primarily limited to minimum feature size (minimum length-scale), however there have been several attempts at maximum length scale.<sup>4,8</sup> Additionally, Guest and Zhu optimized for topologies manufacturable by a milling process.<sup>11</sup> Others have looked at discrete object placement in topologies.<sup>10,13</sup> Gaynor et. al optimized considering the capabilities of a multi-material 3D printer to produce multi-material compliant mechanisms.<sup>6</sup>

## II. Optimization Formulation

Within the realm of topology optimization, the minimum compliance (maximum stiffness) optimization problem is the most common. The component stiffness is a function of the material distribution within a design domain. Each design domain is discretized into a number of finite elements and each element density,  $\rho$ , is allowed to vary from 0-1, where 0 indicates a void and 1 indicates solid material. While the  $\rho$  are allowed to continuously vary between 0 and 1, the end goal is to drive to a binary 0/1 solution. This is achieved through the usual SIMP penalization,<sup>2,18</sup> where intermediate densities are deemed inefficient.

The minimum compliance optimization formulation takes on the following form, seen in Eq. (1).

$$\begin{aligned} \min_{\psi} \quad & f(\psi) = F^T d \\ \text{subject to:} \quad & K(\psi)d = F \\ & \sum_{e \in 1} \rho(\phi(\psi))^e v^e \leq V \\ & 0 \leq \psi^e \leq \psi_{\max}^e = 1 \quad \forall e \in \Omega \end{aligned} \tag{1}$$

where  $\psi$  are the nodal design variables,  $\phi$  are the projected design variables after application of the overhang Heaviside function,  $v^e$  is the elemental volume,  $V$  is the total allowable volume, and  $\Omega$  is the design domain.

Here, there is only one explicit constraint, the volume constraint. The minimum length scale and overhang constraint are imposed through use of clever mapping and projection routines. By imposing the constraints through a projection instead of an explicit constraint, the optimization problem is much easier for the optimizer to solve. Alternatively, the build angle constraint could be imposed as a penalty function. As mentioned before, this was proposed by Brackett et al.,<sup>3</sup> in which he proposed a heuristic penalization scheme on overhangs which violate the maximum allowable angle.

## A. Minimum Lengthscale

The minimum lengthscale control is imposed by a projection of nodal design variables to the physical space.<sup>7</sup> The Heaviside Projection Method (HPM) is imposed to achieve both a minimum lengthscale and eliminate the oft-mentioned checkerboard solution.<sup>7,9</sup> The details are not included here but the general form is seen in Eq. (2)

$$\rho = H(\mu(\phi)) = 1 - e^{\mu(\phi)\beta} + \mu(\phi)e^{-\beta} \quad (2)$$

where  $\mu$  is the weighted average of the design variables within the minimum allowable radius,  $r_{\min}$ , and  $\beta$  is the Heaviside exponent. As  $\beta$  approaches infinity, the continuous approximation to the Heaviside function approaches the discontinuous true Heaviside function.

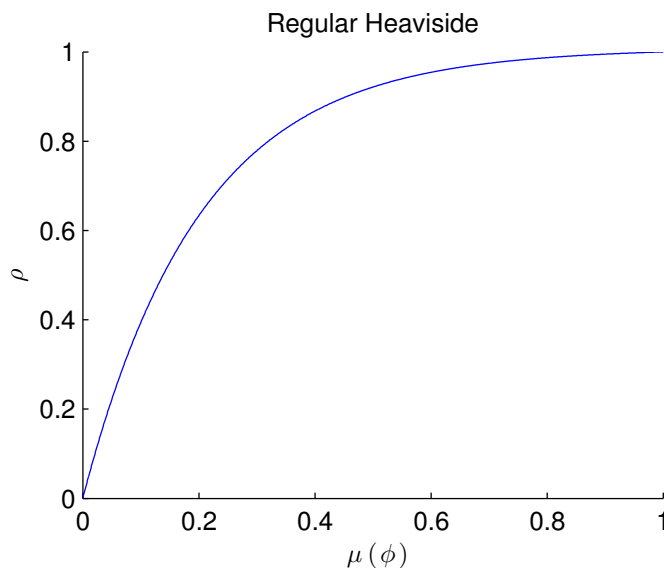


Figure 1: Projection of  $\phi$  to  $\rho$  to achieve minimum length scale (minimum feature size) control.

Others use a similar projection of elemental design variables onto the physical space in order to achieve the same minimum allowable feature size.<sup>1</sup>

## B. Maximum Overhang Control

As stated above, the engineer would like to eliminate the need for support material during the build process. By limiting the overhang of the built part to the observed maximum achievable overhang, support material will be completely eliminated. According to work done by Thomas,<sup>21</sup> the usual maximum achievable overhang for SLM printed parts is around 45 degrees. While this may be the case, the following framework is general enough to optimize for any number of angles.

As in the case of imposing the minimum lengthscale constraint, the build angle constraint is imposed through a mapping and projection of design variables to another set of variables. Therefore, instead of the usual  $\phi \rightarrow \rho$ , we now have a  $\psi \rightarrow \phi \rightarrow \rho$ , where the maximum overhang constraint is imposed in the projection of  $\psi$  to  $\phi$  and the minimum length scale is imposed in the projection of  $\phi$  to the physical space,  $\rho$ .

In the usual minimum compliance with HPM for lengthscale control, the design variables are  $\phi$ . Now the design variables,  $\psi$ , first have to be projected to  $\phi$  before the  $\phi$  can be projected to form the physical space  $\rho$ . At each point, the  $\phi$  check whether they can exist. This is achieved through a strict multiplication scheme in which the local design variable,  $\psi$  is multiplied by an average of the below  $\phi$ . This is seen in Eq. (3).

$$\phi^i = \psi^i \phi_S^i \quad (3)$$

The basic logic is as follows: the above  $\phi$  are not allowed to exist unless adequately supported. Each  $\phi$  scans below at an angle of  $\pm$  the maximum achievable overhang. This is seen in Fig. 2.

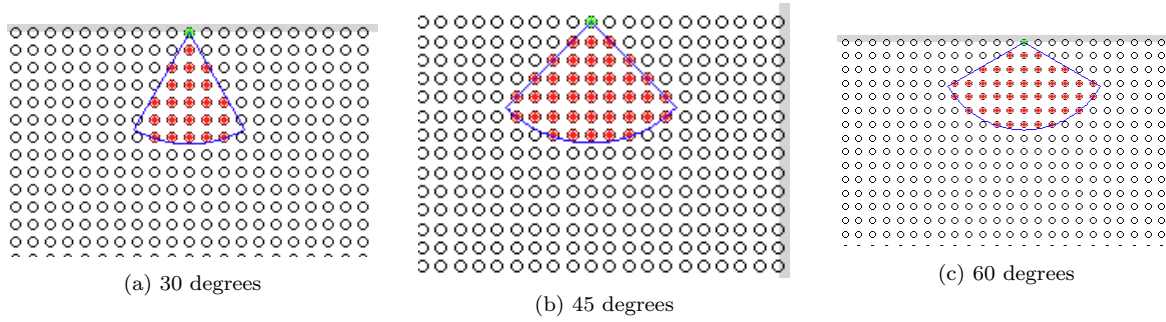


Figure 2: Overhang constraint: scanning range below  $\phi$  for various overhang angles

To determine whether a  $\phi$  is adequately supported, it must be determined what qualifies as minimally fully supported. For example, for the  $45^\circ$  case in Fig. 2b, the maximum overhang case would be along either of the two angles sides. A side has four  $\phi$  and the entire “wedge” has 38  $\phi$ . Therefore, in order for the green  $\phi$  to be supported, the average of the below phi must be at least  $\frac{4}{38} = 0.105$ .

The thresholding Heaviside function, borrowed from Jansen’s robust topology optimization paper,<sup>15</sup> serves as a way of mapping the average of the supporting  $\phi$  to a variable  $\phi_S$ . The averaging operator is designated as  $\mu_{av}$  and is simply the arithmetic mean of the supporting  $\phi$ . This average is mapped to  $\phi_S$  through Eq. (4).

$$\phi_S = H_T(\phi_{in \text{ support wedge}}) = \frac{\tanh(\beta_2 T) + \tanh(\beta_2(\mu_{av}(\phi) - T))}{\tanh(\beta_2 T) + \tanh(\beta_2(1 - T))} \quad (4)$$

where  $\beta_2$  is the Heaviside exponent and  $T$  is the threshold value. As  $\beta_2$  approaches infinity, the smooth Heaviside approximation approaches the true discontinuous Heaviside function. The thresholding Heaviside function is seen in Fig. 3.

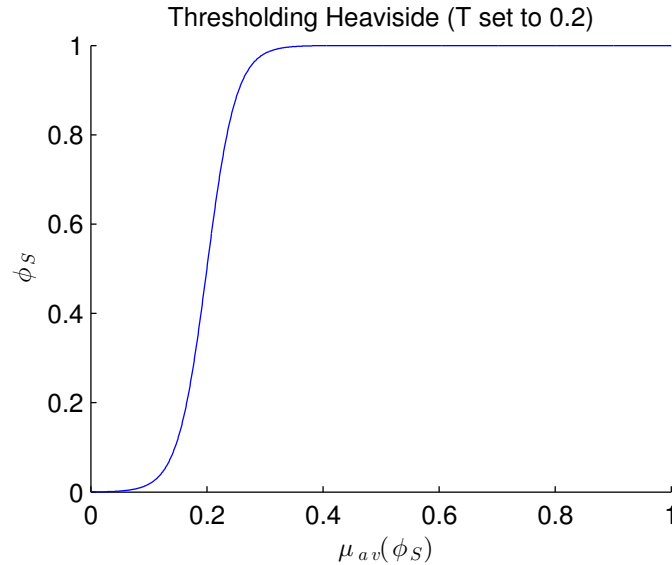


Figure 3: Thresholding Heaviside with threshold,  $T = 0.2$ .

Notice that when the average of supporting  $\phi$  is below the threshold, then  $\phi_S \approx 0$ . Conversely, when the average of supporting  $\phi$  is above the threshold, then  $\phi_S \approx 1$ , allowing the  $\phi$  above to equal 1.

## C. Derivatives and Implementation

While the optimization formulation is now more complicated looking than the typical minimum compliance with HPM for lengthscale control, it still possesses a differentiable objective and constraint function. This problem is implemented using the gradient based Method of Moving Asymptotes (MMA) optimizer.<sup>20</sup>

### 1. Derivatives

The usual derivatives when using HPM are seen in Eq. (5), where the derivative are a straightforward differentiation of the objective function,  $f$  with respect to  $\phi$ .

$$\frac{\partial f}{\partial \psi} = \frac{\partial f}{\partial \rho} \frac{\partial \rho}{\partial \phi} \quad (5)$$

With the addition of the maximum overhang constraint, the derivatives require just have one additional term,  $\frac{\partial \phi}{\partial \psi}$ . They then take on the form seen in Eq. (6)

$$\frac{\partial f}{\partial \psi} = \frac{\partial f}{\partial \rho} \frac{\partial \rho}{\partial \phi} \frac{\partial \phi}{\partial \psi} \quad (6)$$

### 2. Implementation

With the addition of the extra Heaviside function and the strict  $\phi^i = \psi^i \phi_S^i$  rule, the optimization problem becomes highly nonlinear. To help account for this extreme nonlinearity and to stabilize the optimization convergence a continuation scheme is implemented. The continuation is applied to both the SIMP exponent,  $\eta$  and the thresholding Heaviside function's  $\beta_2$  parameter. As  $\eta$  increases, the intermediate volume fraction material becomes less and less efficient, helping the algorithm converge to a 0-1 solution. When  $\beta_2$  increases, the maximum overhang constraint becomes more and more strict as the smooth Heaviside approximation approaches the true Heaviside. As with many topology optimization algorithms, the continuation schemes are necessary to help guide the optimization closer to the global minimum. If the aforementioned parameters are set to high values from the onset, the optimization problem would be highly nonlinear and extremely susceptible to local minima.

Another small detail to consider is the thresholding value,  $T$ . Every  $\phi$  has a unique  $T$  based on the number of  $\phi$  within the arc of supporting  $\phi$ . Those  $\phi$  on the edge of the domain will have about half the number of supporting  $\phi$  as those  $\phi$  in the center of the domain. Currently, the  $T$  is determined by counting the number of supporting  $\phi$  along the maximum support angle and then subtracting a small amount (approximately 0.05). This subtraction is necessary because the  $T$  value in Eq. (4) indicates the middle point of the incline. However, it is desired to have  $\phi_S$  equal to 1 when the number of supporting  $\phi$  is adequate, therefore requiring a slight shift to the left of the thresholding heaviside.

## III. Solutions

The algorithm is tested on two typical topology optimization problems, the MBB beam seen in Fig. 4 and the cantilever beam seen in Fig. 5 where the grey region indicates the design domain.

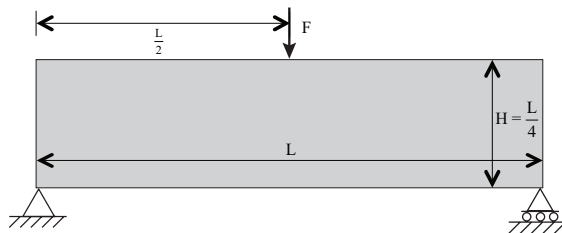


Figure 4: MBB beam definition.

First, solutions for the usual minimum compliance subject to only the minimum lengthscale control are presented (Fig. 6 and Fig. 7). These solutions are widely known and are shown for comparison purposes. Red indicates solid while blue indicates void.

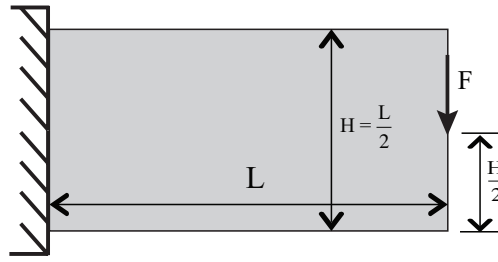
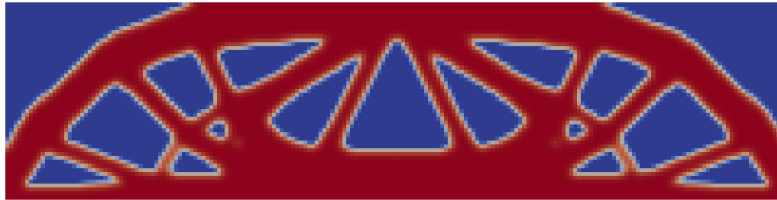


Figure 5: Cantilever beam definition.

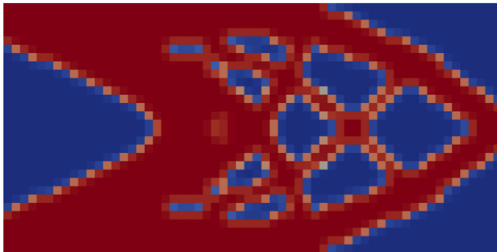


(a) Simply supported beam solution: no maximum angle constraint.

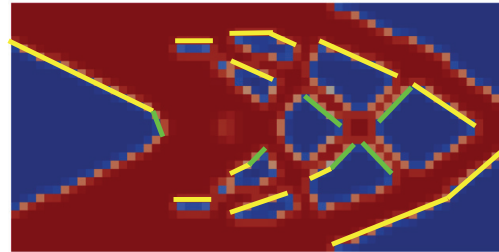


(b) Green indicates allowable overhang while yellow indicates a violation of the overhang rule.

Figure 6: Minimum compliance solution to MBB beam problem with no overhang constraint.



(a) Cantilever beam solution: no maximum angle constraint.



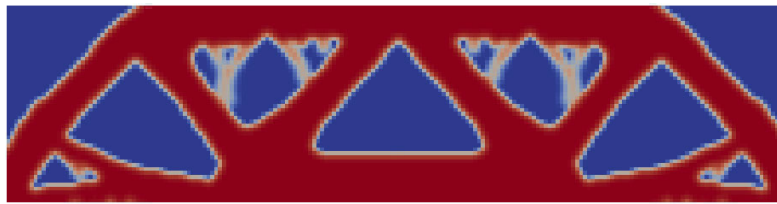
(b) Green indicates allowable overhang while yellow indicates a violation of the overhang rule.

Figure 7: Minimum compliance solution to cantilever beam problem with no overhang constraint.

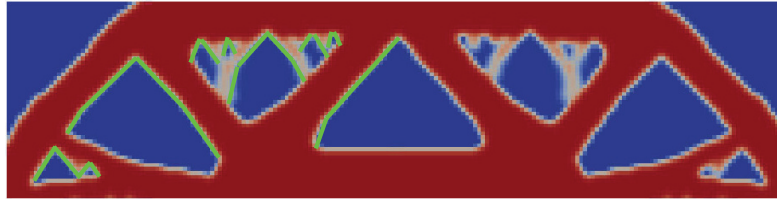
If it is imagined that the structures must be build from the bottom up, then these conventional solutions violate the  $45^\circ$  maximum allowable overhang and would require support structures during the build process. This violation is highlighted in Fig. 6b and Fig. 7b, where the green lines indicate an overhang angle of  $< 45^\circ$  while the yellow lines indicate an overhang angle of  $> 45^\circ$ .

Now, the same MBB beam and cantilever beam problems are optimized using the maximum overhang optimization formulation. This algorithm will not allow material to exist unless it is supported at an angle of  $45^\circ$  or less from vertical. As can be seen in the solution for the MBB beam subject to the overhang constraint (Fig. 8b), every part of the topology is supported by material at an angle of  $\pm 45^\circ$ .

The cantilever problem was also solved subject to the  $45^\circ$  maximum overhang constraint. As can be seen in Fig 9b, almost all of the overhangs in the solution (one small exception) adhere to the constraint.

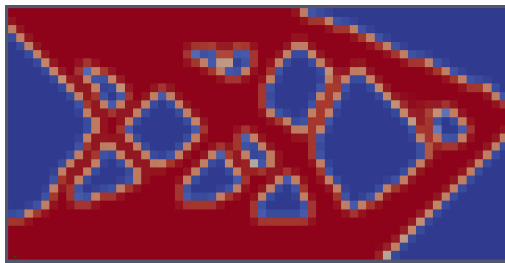


(a) Simply supported beam solution: 45 deg maximum angle constraint.

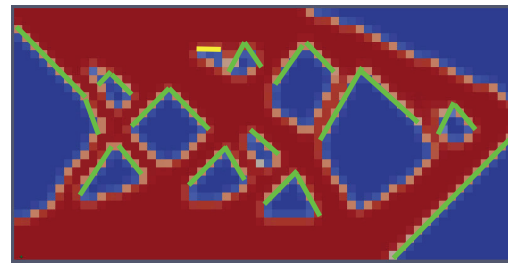


(b) Green indicates allowable overhang while yellow indicates a violation of the overhang rule.

Figure 8: Minimum compliance solution to MBB beam problem with 45 deg overhang constraint.



(a) Cantilever beam solution: no maximum angle constraint.



(b) Green indicates allowable overhang while yellow indicates a violation of the overhang rule.

Figure 9: Minimum compliance solution to cantilever beam problem with no overhang constraint.

There are, however, some small convergence issues present in the current solutions. This is especially noticeable in the MBB beam example (Fig. 8), where there are some intermediate density elements, especially those supporting the thick horizontal member on the top of the domain. To help solve this issue, a smarter continuation scheme should be developed. It is necessary to increase the  $\beta_2$  parameter as much as possible without simultaneously making the optimization problem too nonlinear to solve for a feasible solution.

Also of concern is the choosing of the threshold parameter,  $T$ . As stated before, the value must be adjusted such that when there are an adequate number of supporting  $\phi$ , the algorithm will allow the  $\phi_S$  to be one. The algorithm is fairly sensitive to this value  $T$ , as changing the value by too much can impose an inaccurate angle constraint.

## IV. Conclusion

This paper proposes using topology optimization for the design of additively manufactured components which contain overhangs only up to the maximum achievable overhang. By limiting the overhangs to achievable angles, sacrificial support material is eliminated from the design process, saving time and money. The proposed method borrows ideas from previous projection methods by adding an additional projection to the optimization scheme. In this way, the overhang constraint is imposed without adding an explicit constraint to the optimization problem.

Examples cases are shown for both the MBB beam problem and the cantilever beam problem. Traditional topology optimization solutions to these problems possess many violations of the overhang constraint while solutions subject to the overhang constraint possessed little or no violations. The overhang optimization

algorithm proves to be fairly nonlinear, however when care is taken to adopt smart continuation schemes, the optimizer can drive towards converged solutions.

## Acknowledgments

The lead author gratefully acknowledges support from the National Science Foundation (NSF) IGERT Program (DGE-0801471). The authors also thank Krister Svanberg for providing the MMA optimizer code.

## References

- <sup>1</sup>Bendsøe, M.P., and Sigmund, O., *Topology Optimization: Theory, Methods and Applications*. Springer, Berlin, 2003.
- <sup>2</sup>Bendsøe, M.P., Optimal shape design as a material distribution problem (1989) *Structural Optimization*, 1 (4), pp. 193-202.
- <sup>3</sup>Brackett, D., Ashcroft, I., Hague, R., Topology optimization for additive manufacturing (2011) 22nd Annual International Solid Freeform Fabrication Symposium - An Additive Manufacturing Conference, SFF 2011, pp. 348-362.
- <sup>4</sup>Carstensen, J.V., Guest, J.K., New Projection Methods for Two-Phase Minimum and Maximum Length Scale Control in Topology Optimization, 15th AIAA/ISSMO Multidisciplinary Analysis and Optimization Conference, 2014
- <sup>5</sup>Cloots, M., Spierings, A.B., Wegener, K., Assessing new support minimizing strategies for the additive manufacturing technology SLM, (2013) 24th International SFF Symposium - An Additive Manufacturing Conference, SFF 2013, pp. 631-643.
- <sup>6</sup>Gaynor, A.T., Meisel, N.A., Williams, C.B., Guest, J.K., Multiple-Material Topology Optimization of Compliant Mechanisms Created Via PolyJet 3D Printing, *ASME J. Manuf. Sci. Eng.*, (in review)
- <sup>7</sup>Guest, J.K., Prévost, J.H., Belytschko, T., Achieving minimum length scale in topology optimization using nodal design variables and projection functions (2004) *International Journal for Numerical Methods in Engineering*, 61 (2), pp. 238-254.
- <sup>8</sup>Guest, J.K., Imposing maximum length scale in topology optimization (2009) *Structural and Multidisciplinary Optimization*, 37 (5), pp. 463-473.
- <sup>9</sup>Guest, J.K., Topology optimization with multiple phase projection, *Computer Methods in Applied Mechanics and Engineering*, Vol. 199, 2009, pp. 123-135.
- <sup>10</sup>Guest, J.K., Igusa, T. "A Projection-Based Topology Optimization Approach to Distributing Discrete Features in Structures and Materials", 9th World Congress on Structural and Multidisciplinary Optimization, 2011, pp.1-10.
- <sup>11</sup>Guest, J.K., Zhu, M. Casting and Milling Restrictions in Topology Optimization via Projection-Based Algorithms. *Proceedings of the ASME Design Engineering Technical Conference*, 3 (PARTS A AND B), 913-920, (2012)
- <sup>12</sup><http://www.stratasys.com/3d-printers/technologies/fdm-technology/>. Stratasys FDM system. Accessed 05-22-14.
- <sup>13</sup>Ha, S., Guest, J.K., Optimizing inclusion shapes and patterns in periodic materials using Discrete Object Projection, *Struct. Multidisc. Optim.*, (in press)
- <sup>14</sup>Hussein, A., Hao, L., Yan, C., Everson, R., Young, P., Advanced lattice support structures for metal additive manufacturing (2013) *Journal of Materials Processing Technology*, 213 (7), pp. 1019-1026.
- <sup>15</sup>Jansen, M., Lombaert, G., Diehl, M., Lazarov, B.S., Sigmund, O., Schevenels, M., Robust topology optimization accounting for misplacement of material (2013) *Structural and Multidisciplinary Optimization*, 47 (3), pp. 317-333.
- <sup>16</sup>Mercelis, P., Kruth, J.-P. Residual stresses in selective laser sintering and selective laser melting, (2006) *Rapid Prototyping Journal*, 12 (5), pp. 254-265.
- <sup>17</sup>Mumtaz, et al. (2011), "A method to eliminate anchors/supports from directly laser melted metal powder bed processes", Presented at Solid Freeform Fabrication, Texas, University of Texas.
- <sup>18</sup>G.I.N. Rozvany, M. Zhou, T. Birker, Generalized shape optimization without homogenization, *Struct. Optim.* 4 (1992) 250252.
- <sup>19</sup>Sigmund, O., and Petersson, J., Numerical instabilities in topology optimization: a survey on procedures dealing with checkerboards, mesh-dependencies and local minima, *Structural Optimization* Vol. 16, 1998, pp. 68-75.
- <sup>20</sup>Svanberg, K., METHOD OF MOVING ASYMPTOTES - A NEW METHOD FOR STRUCTURAL OPTIMIZATION. (1987) *International Journal for Numerical Methods in Engineering*, 24 (2), pp. 359-373.
- <sup>21</sup>Thomas, T. (2009). *The Development of Design Rules for Selective Laser Melting*. Ph.D. Thesis. University of Wales Institute, Cardiff: U.K.
- <sup>22</sup>Vandenbroucke, B., Kruth, J., Selective laser melting of biocompatible metals for rapid manufacturing of medical parts, (2007) *Rapid Prototyping Journal*, 13 (4), pp. 196-203.
- <sup>23</sup>Xu, C., Chai, W., Huang, Y., Markwald, R.R., Scaffold-free inkjet printing of three-dimensional zigzag cellular tubes, (2012) *Biotechnology and Bioengineering*, 109 (12), pp. 3152-3160.